PRECIPITATION IN A Cu-BASED SMA①

Chang, Fenglian Wang, Shidong Wang, Yurui Zhao, Liancheng
Analytical and Testing Center, Southeast University, Nanjing 210018

ABSTRACT The morphology, composition and crystal structure of the precipitation in a Cu-Zn-Al-Mn-Ni-Ti shape memory alloy have been studied. The results indicated that there were two different second phase particles in the as-quenched microstructure: a large irregular-shaped X_L phase and a fine dispersed X_S phase, both of which were ordered $L2_1$ b.c.c. structure with the composition $(CuNiFe)_2TiAl$. For the case of X_S, the lattice parameter $a(X_S)=0.5879$ nm. With low solution-treatment temperature and short treatment time, the X_S phase was fine dispersed and coherent to the matrix, nevertheless, the coherency would be destroyed by the growth of X_S phase as treatment temperature and time increasing.

Key words: crystal structure shape memory second phase

1 INTRODUCTION

By adding trace elements to refine grains, the cold workability and fatigue properties of polycrystalline Cu-based Shape Memory Alloys (SMA) can be markedly improved[1-2]. According to reports, presnetly, Fe[3] and Ti[4] are commonly adopted as grain refinement agents for Cu-Al-Ni alloys, while Zr[5], B[6] and V[7] are adopted for Cu-Zn-Al alloys. Each refinement agent produces different effect. It is generally believed that Ti addition can refine the grains by forming second phase in the matrix, which hinders the growth of grains and consequently improves the properties of the alloy. However, neither the morphology structure of the second phase nor refinement mechanism has been clarified. In this paper, investigation and discussion regarding these problems have been made by optical microscopy, electron probe microanalysis and transmission electron microscopy.

2 EXPERIMENTAL

The alloy of the composition Cu-13.47Zn-5.89Al-5.00Mn-0.97Ni-0.64Ti (wt. -%) had been melted in an induction furance. The ingot was homogenized at 850 ℃ for 5 h, forged to plates, hot rolled to 2.0~2.5 mm in thickness, and then cold rolled to 1.0~1.5 mm in thickness. Specimens for measuring martensitic transformation temperature were subject to solution treatment at 830 ℃ for 20 min, and quenched into oil. The measurement result was $M_s=50$ ℃, $M_f=22$ ℃, $A_s=40$ ℃, $A_f=66$ ℃.

TEM observations and EDX analysis were carried out using Philips-CM12 electron microscope operated at 120 kV. TEM foils were prepared by double jet electropolishing using an electrolyte containing 30% nitric acid and methanol. Composition analysis and morphology observation of the X phase in as-cast specimen and the X_L phase in as-quenched specimen were made on Jeol Superprobe 733 using operating voltage 20 kV.

3 RESULT AND DISCUSSION

3.1 *Feature of the X Phase*

As shown in Fig. 1, the metallography of as-cast specimen is composed of phases of the white needlelike α, black matrix β and X, which locates between α and β. According to its back-reflection electron image (Fig. 2), the X phase is irregular-shaped and uniformly distributed in the matrix. The results of electron

① Received Dec. 25, 1993; accepted in the revised form Feb. 28, 1994

probe microanalysis (Table 1)indicate that the X phase is mainly composed of Cu, Ni, Fe, Ti and Al with atomic percentage close to (Cu+Ni+Fe) : Ti : Al = 2 : 1 : 1. The negligible Zn and Mn are assumed to be arisen from analysis deviation effected by the matrix. In addition, Fe may be introduced from electrolytic Mn and interalloy containing Ti.

3. 2 *Structure and Composition of the X_L and X_S Phases*

The two particle phases, irregular-shaped large X_L and fine dispersed X_S, are found in as-quenched microstructure which are shown in Fig. 3(a) and 3(b), respectively. As indicated in Table 2, the composition of X_L is close to $(CuNiFe)_2TiAl$, which conforms to that of the X phase in as-cast specimen, suggesting that the X_L phase in as-quenched specimen forms from the transition of the X phase in as-cast specimen. For sake of comparison, the matrix composition around the X_L phase, which mainly are Cu, Zn, Al and Mn, is also given in Table 2. Adachi *et al*[8] had found an X_L phase of a composition $(CuNi)_2TiAl$ in Cu-Al-Ni-Ti alloys and determined its structure as $L2_1$ ordered b. c. c. By comparison, it is believed that the two X_L phases are essentially identical, except that the X_L phase in this paper contains a minute amount of dopant Fe, which replaces partial Ni that occupies site I of DO_3

Table 1 Composition of the X phase in as-cast specimen

Elements	Cu	Zn	Al	Mn
at. %	27.568	0.877	24.234	1.468
Elements	Ni	Ti	Fe	
at. %	15.694	24.237	5.922	

Fig. 1 As-cast optical micrograph of the alloy

Fig. 2 Micrograph of X phases in as-cast microstructure

Fig. 3 Micrograph of X_L (a) and X_S (b) phases in as-quenched microstructure

Table 2 Composition of the X_L phase and matrix around it

Elements	Cu	Zn	Al	Mn
X_L (at. -%)	26.915	0.563	23.935	1.632
Matrix (at. -%)	68.113	12.154	13.023	5.568

Elements	Ni	Ti	Fe
X_L (at. -%)	16.523	23.813	6.620
Matrix (at. -%)	0.717	0.299	0.126

structure in the X_L phase found by Adachi.

Fig. 4(a) shows the morphology of the X_S phase in specimen experienced heat treatment at 900 ℃ for 1 h. Its μ- diffraction patterns along [100], [110] and [$\bar{1}$11] are shown in Fig. 4(b) ~ (d), indicating a DO_3 structure with lattice parameter $a(X_S) = 0.5879$ nm, which is close to that of the X_L phase[8].

X-ray EDAX analysis result for different X_S phase is shown in Table 3, just as that of X_L, its atomic percentage can be describe as $(CuNiFe)_2TiAl$, suggesting that of X_S phase has also an ordered $L2_1$ structure. The model in Fig. 5 has schemically described the structure of X_S: Cu, Ni and Fe occupy site I while Ti and Al occupy site II and III, respectively.

3.3 *Relationship Between X_S, X_L and Matrix*

As indicated by Adachi *et al*[8], when the alloy experiences heat treatment in β phase region, the X phase in as-cast microstructure transforms to X_L, and at the time, precipitates X_S. TEM study shows that there is no determined orientation relationship between X_L and the matrix, and the morphology and dimension of X_S vary with the temperature and time of solution treatment. With low treatment temperature and short annealing time, the X_S phase is

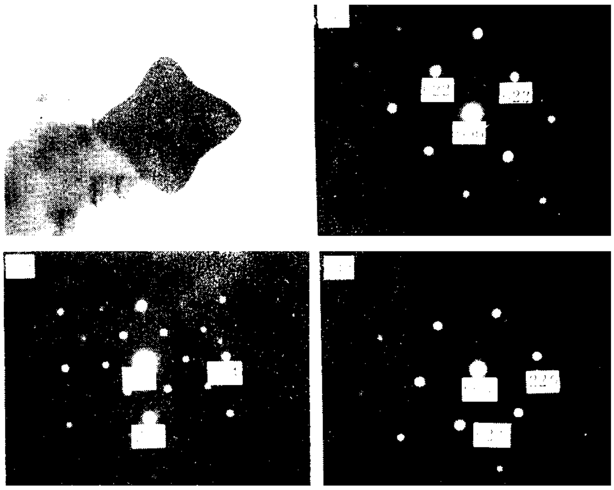

Fig. 4 Morphology of the X_S phase (a), and its μ- diffraction pattern, showing a $DO_3/L2_1$ structure, (b) [100], (c) [110], (d) [$\bar{1}$11]

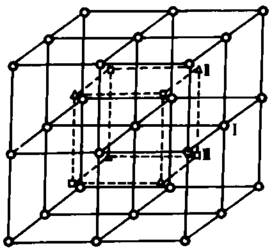

Fig. 5 Unit cell of the $L2_1$ structure of the X_S phase.
Sublattice sites I, II and III are occupied by (Cu or Ni or Fe), Ti and Al, respectively

Table 3 Atomic percentage of the X_S phase

Elements	Cu	Zn	Al	Mn
at.-%	28.359	1.928	21.420	1.869
Elements	Ni	Ti	Fe	
at.-%	16.201	23.727	6.496	

nearly sphere in shape, dispersing uniformly in the matrix.

Because of their identical crystal structure, small lattice misfit degree ($\delta = 0.14\%$) and the fine dispersed distribution of X_S, at the initial precipitation stage, it can be presumed that the X_S phase and matrix are coherent. Fig. 6(a) shows the bright-field image of the X_S phase and the matrix with operating vector $\vec{g}_1 = (220)^*$, noncontrast line in X_S appears, and its direction changes as the operating vector changes to $\vec{g}_2 = (224)^*$, indicating that at the initial precipitation stage, the X_S phase is coherent to the matrix. This coherency will be destroyed upon the growth of X_S.

3.4 *Discussion on Refinement*

The doped Ti refines the microstructures of as-cast, hot-rolled and as-quenched specimens of the alloy. The mechanism is discussed as follows:

3.4.1 Refinement of as-cast microstructure

According to Adachi[9], Ti addition changes the solidification processes of the alloy. In cooling process, β phase crystallizes from the liquid state at first, and at a certain temperature, eutectic transformation $L \to \beta + X$ takes place. Compared with that without refinement agent, as-cast microstructure of Cu-based SMA with Ti addition refines evidently due to the eutectic transformation. In addition, because of the formation of the X phase arising from the strong affinity between Ni, Al and Ti, the diffusion rate of the atoms in the alloy decreases, resulting in a finer microstructure.

3.4.2 Refinement of hot-rolled microstructure

For hot-rolled specimens, the heavy plastic deformation and the subsequent recrystallization annealing can effectively refine the microstructure. By adding Ti, $(CuNiFe)_2TiAl$

Fig. 6 Matrix strain field contract
(a)—$\vec{g}_1 = (220)^*$; (b)—$\vec{g}_2 = (224)^*$

phase forms, which suppresses the coarsing of recrystallization grain, resulting in a finer microstructure.

3. 4. 3 Refinemnet of the as-quenched microstructure

The fine dispersed X_S in as-quenched microstructure not only affects the diffusion rate of the atoms in the alloy, but also pins the interface. So it will hinder the growth of grains. The smaller the X_S is and the more dispersed it distributes, the stronger the pinning will be.

Thus, Ti additon refines the microstructure by three ways: (1) eutectic transformation at initial stage of solidification; (2) low atom diffusion rate and (3) the fine dispersed X_S, which hinders the growth of the grains.

4 CONCLUSIONS

(1) The as-quenched Cu-Zn-Al-Mn-Ni-Ti shape memory alloy contains two different shaped particles: irregular-shaped large X_L and fine dispersed X_S, both of them are ordered $L2_1$ b. c. c. structure with composition $(CuNiFe)_2TiAl$. For the case of X_S, lattice parameter is 0. 5879 nm.

(2) There is no determined orientation relationship between the X_L phase and matrix. With low solution treatment temperature and short treatment time, the X_S phase is fine dispersed and coherent to the matrix. Nevertheless, the coherency will be destroyed upon the growth of the X_S phase as the treatment temperature and the time increase.

REFERENCES

1 Sure, GN; Brown, LC. Met Trans, 1984, 15A: 1613.
2 Sure, GN; Brown, LC. Scripta Metall, 1985, 19: 401.
3 Hasan, F; Lorimer, GW *et al.* J de Physique, 1982, 43: C4-653.
4 Elst, R; Humbeeck, J; Melus, M; Delaey, L. Z Metallkde, 1986, 77: 421.
5 Lee, JS; Wayman, CM. Metallography, 1986, 19: 401.
6 Enami, K; Takimoto, N *et al*, J de Physique, 1982, 43: C4-773.
7 Han, YS *et al.* Scripta Metall, 1987, 21: 947.
8 Adachi, K *et al.* Scripta Metall, 1987, 21: 453.
9 Adachi, K; Shoji, K. In: Proc of the MRS Intl Meet on Adv Mater. Tokyo: The Materials Research Society, 1988, 365.